$O^{16}(p,\alpha)N^{13}$ and $O^{16}(p,p')O^{16*}$ Differential Cross Sections*

R. L. DANGLE,† L. D. OPPLIGER,‡ AND G. HARDIE§
University of Wisconsin, Madison, Wisconsin
(Received 5 September 1963)

The differential cross sections for the inelastic scattering of protons by O^{16} and for the $O^{16}(p,\alpha)N^{13}$ reaction were measured for E_p from 7.18 to 12.90 MeV. A differentially-pumped gas scattering chamber with a solid-state detector was used. Data at $\theta_{lab}=166°\ 00'$ were taken in energy steps $\leqslant 5$ keV and with a target thickness $\leqslant 3$ keV. Seven other excitation curves were taken for $7.18\leqslant E_p\leqslant 10.5$ MeV at $\theta_{lab}=133°\ 48'$, $116°\ 34'$, $100°\ 19'$, $86°\ 24'$, $61°\ 36'$, $51°\ 25'$, and $33°\ 47'$. These curves were taken with energy steps $\leqslant 23$ keV depending upon the width of the resonance structure. The target thickness was $\leqslant 3$ keV. Data were obtained on the alphas leaving N^{13} in its ground state and on the inelastic protons leaving O^{16} in its first, second, third, and fourth excited states. Evidence was found for the existence of 36 levels in F^{17}, the compound nucleus. Below $E_p=10.5$ MeV, center-of-mass angular distributions were picked from the eight excitation curves and fitted with Legendre polynomials. Levels in F^{17} at the following excitation energies were assigned total widths, spins, and parities as indicated: $E_x=7.73$ MeV, $\Gamma_{c.m.}=0.178$ MeV, $J^\pi=\frac{1}{2}^+$; 8.07, 0.104, $\frac{5}{2}^+$; 8.2, 0.706, $\frac{3}{2}^-$; 8.38, 0.011, $\frac{5}{2}^-$; 8.42, 0.042, $\frac{7}{2}^+$; 8.72, 0.188, $\frac{5}{2}^+$; 8.95, 0.122, $\frac{5}{2}^-$; 9.16, 0.188, $\frac{3}{2}^+$; 10.05, 0.282, $\frac{7}{2}$. All parity assignments except those for the levels at $E_x=8.95$ and 9.16 MeV are based on the assumption that the F^{17} level at $E_x=8.2$ MeV is the mirror of the $\frac{3}{2}^-$ level in O^{17} at $E_x=7.72$ MeV.

INTRODUCTION

SEVERAL investigations of the level structure of F^{17} have been made at Wisconsin using protons elastically scattered by O^{16}.[1–6] The data obtained provided approximate resonant energies and widths for levels in the energy region $E_p=0.28$–13.6 MeV. A phase-shift analysis of the data from $E_p=2.0$ to 7.6 MeV yielded additional level parameters in this energy region.[5] Since other particle channels are open above $E_p=5.5$ MeV, the phase-shift analysis became uncertain and was discontinued at $E_p=7.6$ MeV. Preliminary data were taken on these other open channels but the data were not extensive enough to allow a continuation of the phase-shift analysis. However, the off-resonant elastic data were reasonably well fitted by an optical-model analysis.[6]

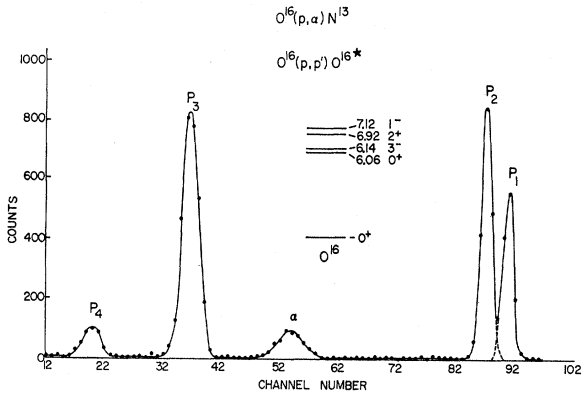

FIG. 1. Pulse-height spectrum obtained with solid-state detector at $E_p=8.87$ MeV, $\theta_{lab}=166°$. The groups labeled P_i refer to inelastic protons leaving O^{16} in its ith excited state. The group labeled α corresponds to alphas leaving N^{13} in its ground state. The elastic proton group is not shown.

This paper reports a detailed investigation of the $O^{16}(p,\alpha)N^{13}$ reaction and the inelastic scattering of protons by O^{16}. Differential cross sections were measured at $\theta_{lab}=166°$ for $E_p=7.18$–12.90 MeV and at seven other laboratory angles for energies up to $E_p=10.5$ MeV. Angular distributions obtained from these excitation curves were fitted with Legendre polynomials. Level parameters obtained from the Legendre polynomial analysis in the energy region $E_p=7.5$–10.5 MeV are reported.

EXPERIMENTAL

Apparatus

A tandem Van de Graaff accelerator was used in conjunction with the small-volume differentially-pumped gas scattering chamber described in Refs. 4 and 8. Only modifications to the chamber made for this experiment will be described here.

During preliminary work a leakage current of 5×10^{-10} A was noted in the charge collecting system. It was found that this current was caused by positive ions striking the back of the collector cup. The positive ions came from the VacIon pump[7] which was used to evacuate the collector cup region. A baffle placed in the throat of the pump eliminated the current. Cross

* Work supported by the U. S. Atomic Energy Commission.
† Present address: University of Sao Paulo, Sao Paulo, Brazil.
‡ Present address: Western Michigan University, Kalamazoo, Michigan.
§ Present address: Armour Research Foundation, Chicago 16, Illinois.
[1] R. A. Laubenstein, M. J. W. Laubenstein, L. J. Koester, and R. C. Mobley, Phys. Rev. **84**, 12 (1951).
[2] R. A. Laubenstein and M. J. W. Laubenstein, Phys. Rev. **84**, 18 (1951).
[3] F. Eppling, Ph.D. thesis, University of Wisconsin, 1953 (unpublished).
[4] S. R. Salisbury, G. Hardie, L. Oppliger, and R. Dangle, Phys. Rev. **126**, 2143 (1962).
[5] S. R. Salisbury and H. T. Richards, Phys. Rev. **126**, 2147 (1962).
[6] G. Hardie, R. L. Dangle, and L. D. Oppliger, Phys. Rev. **129**, 353 (1963).
[7] Varion VacIon pump, Model No. 911-0000.

sections measurements[4,6] which were made with this chamber before insertion of the baffle may be systematically low by as much as 0.5% due to the leakage current.

In order to obtain the energy resolution necessary to separate closely spaced inelastic proton groups, the detecting system previously used[4,6,8] was replaced by one having a smaller angular acceptance ($<3.6°$) and employing a solid-state detector. With this arrangement it was possible to resolve almost completely the inelastic proton groups corresponding to O^{16} being left in its first and second excited states. These two states are separated by only 80 keV. Other inelastic proton groups

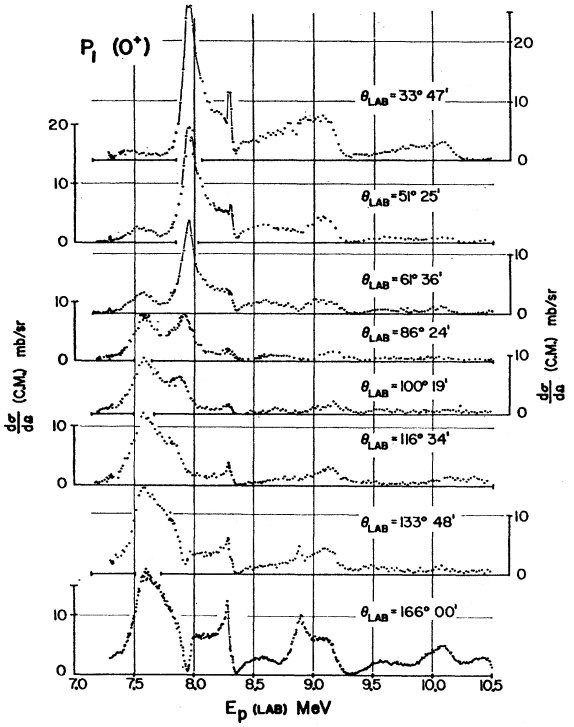

FIG. 2. Excitation curves for protons leaving O^{16} in its first excited state.

and the alphas from the $O^{16}(p,\alpha)N^{13}$ reaction were completely resolved. Pulses from the solid-state detector were analyzed using a multichannel pulse-height analyzer. A pulse-height spectrum is shown in Fig. 1.

Procedure

The relative energy of the alpha particles and the inelastic protons varies strongly as a function of angle and bombarding energy. Because of this, there were energy regions in each excitation curve where the alpha group overlapped one of the inelastic proton groups in

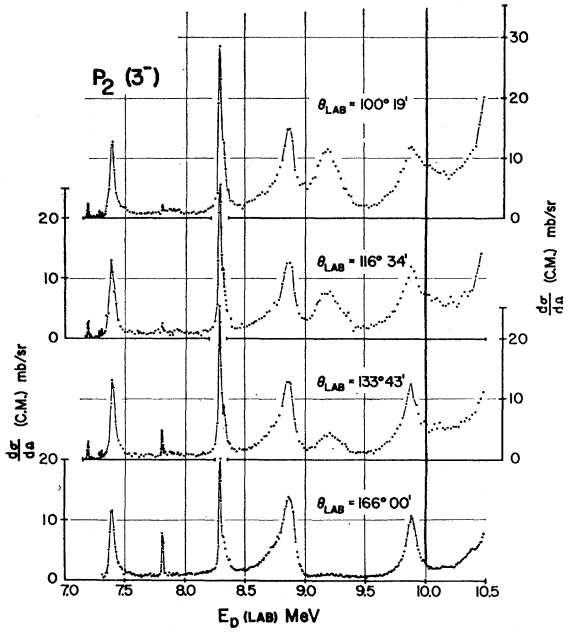

FIG. 3. Excitation curves for protons leaving O^{16} in its second excited state.

the pulse-height spectrum. This difficulty was overcome by exploiting the difference in dE/dx for equal energy protons and alphas. In these regions the proton and alpha groups were separated in the pulse-height spec-

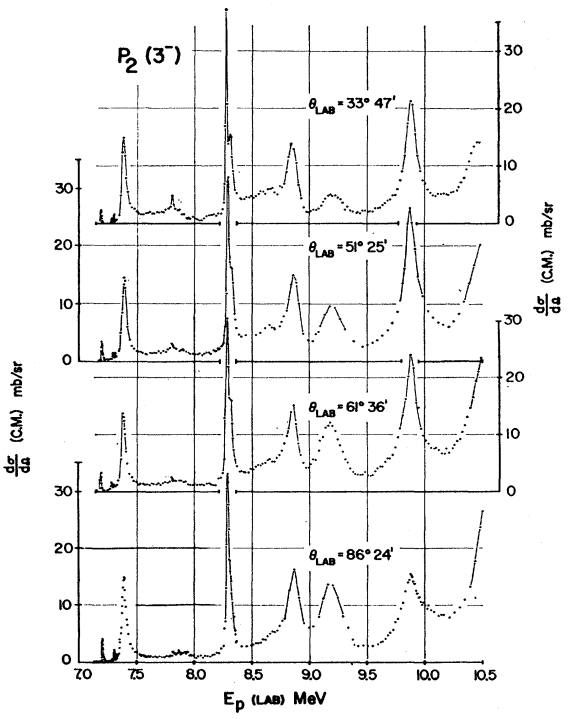

FIG. 4. Excitation curves for protons leaving O^{16} in its second excited state.

[8] E. A. Silverstein, S. R. Salisbury, G. Hardie, and L. D. Oppliger, Phys. Rev. **124**, 868 (1961).

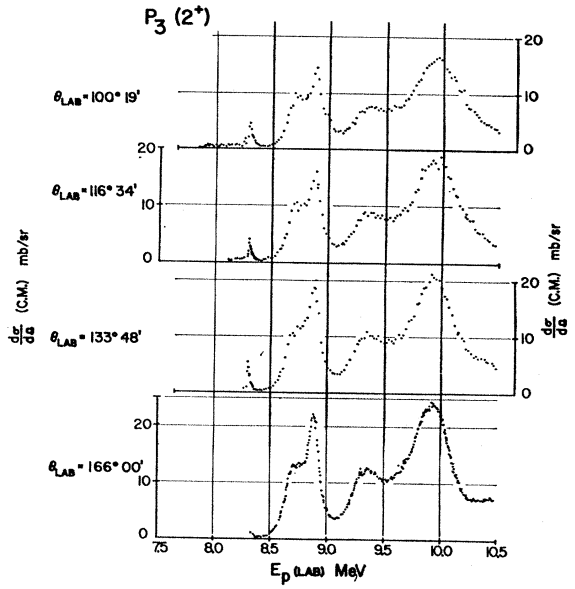

FIG. 5. Excitation curves for protons leaving O^{16} in its third excited state.

trum by varying the target gas pressure or by placing a thin nickel foil (0.0005 mm) directly in front of the detector. As can be seen in Fig. 1, p_1 and p_2 were not completely resolved. The groups were decomposed graphically by plotting each pulse-height spectrum over p_1 and p_2, and drawing a symmetric curve for the more well-defined group. The yield for each group was then read from the plots. This decomposition introduces an uncertainty of approximately 0.2 mb/sr in the cross sections for p_1 and p_2.

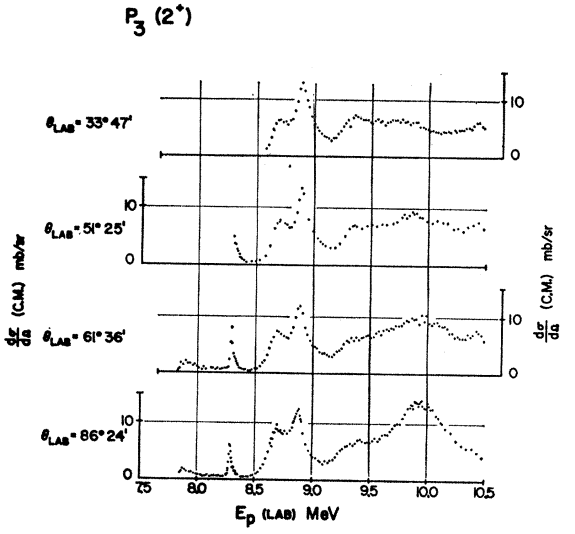

FIG. 6. Excitation curves for protons leaving O^{16} in its third excited state.

Uncertainties

The center-of-mass differential cross section is given by

$$\frac{d\sigma}{d\Omega}(\text{c.m.})=\frac{Y\sin\theta}{NnG}\left(\frac{\sin\theta}{\sin\phi}\right)^2\cos(\phi-\theta),$$

where

$$\sin(\phi-\theta)=\sin\theta\left[\frac{m_1m_3}{m_2m_4}\left(1+\frac{m_1+m_2}{m_2}\frac{Q}{E_p}\right)^{-1}\right]^{1/2},$$

Y is the number of particles detected, N is the number of incident protons, n is the number of target nuclei per cm^3, G is the geometric factor of the counter aperture system,[9] θ is the laboratory angle of observation,

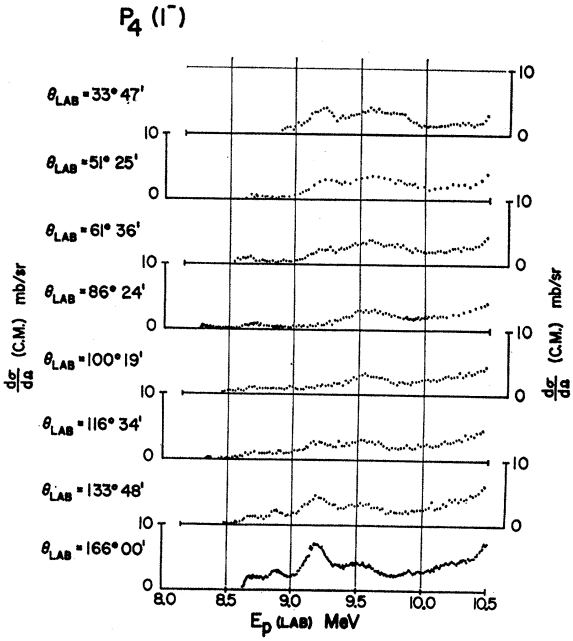

FIG. 7. Excitation curves for protons leaving O^{16} in its fourth excited state.

and ϕ is the corresponding center-of-mass angle. $Q=(m_1+m_2)c^2-(m_3+m_4)c^2$, and m_1, m_2, m_3, and m_4 are the masses of the incident projectile, target nucleus, reaction particle, and residual nucleus, respectively.

The uncertainty in N is $\pm 0.3\%$, the uncertainty in n is $\pm 0.14\%$, and the uncertainty in G is $\pm 0.9\%$. The uncertainty in the laboratory scattering angle is $\pm 6'$. The statistical uncertainty in the yield varies from $\pm 1.2\%$ at the largest cross sections to $\pm 25\%$ at the smallest cross sections. The background subtraction introduces an uncertainty in the cross sections of up to 5% in the lowest 100 keV of each excitation curve. Otherwise the uncertainty due to the background subtraction is less than 1%.

In addition, because of a $\sim 0.26\%$ H_2 impurity and

[9] E. A. Silverstein, Nucl. Instr. Methods, 4, 53 (1959).

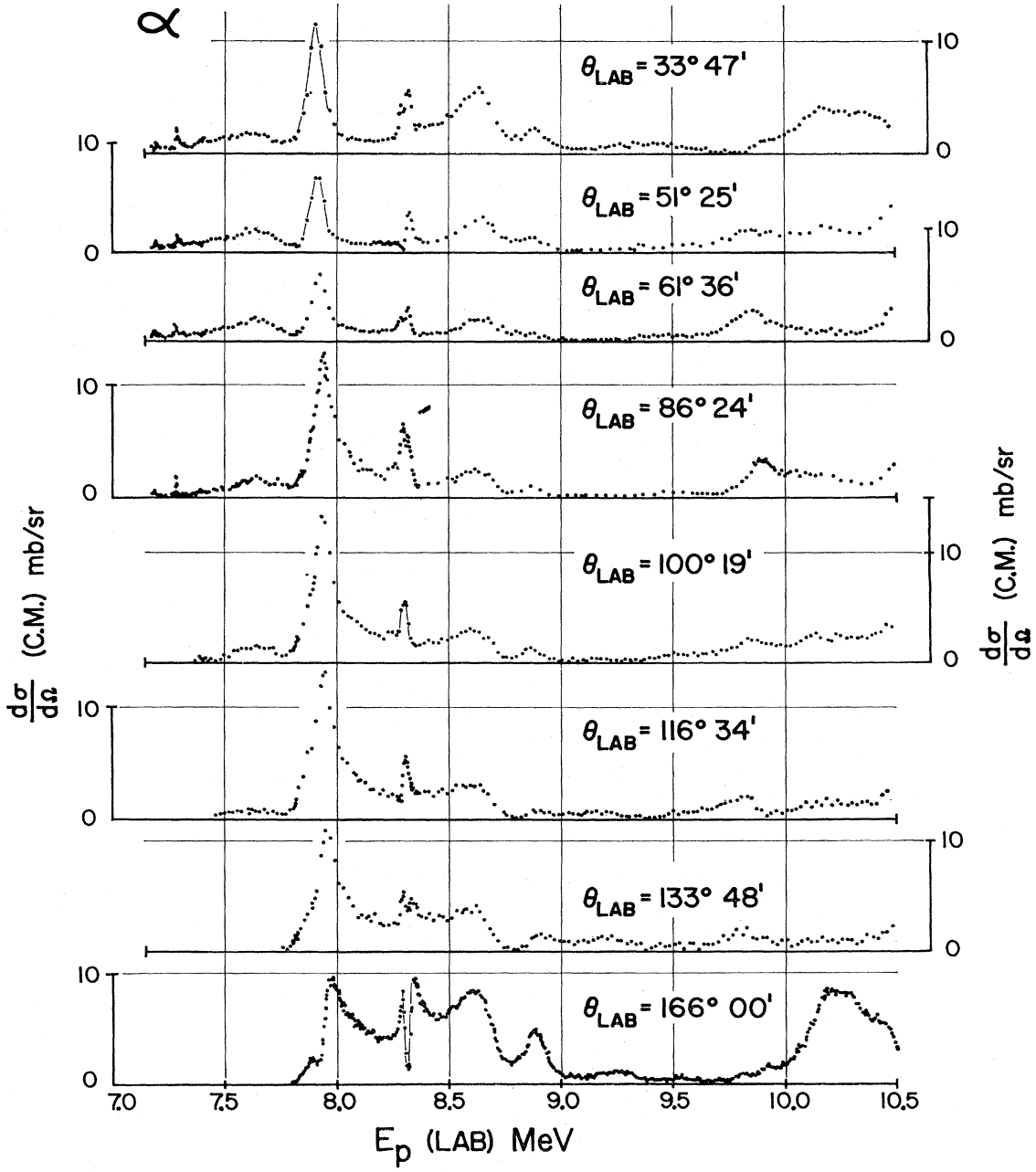

FIG. 8. Excitation curves for alphas leaving N^{13} in its ground state.

a ~0.26% N_2 impurity found after the $\theta_{lab}=166°$ excitation curve was completed, these cross sections are low by ~0.52%. Since the H_2 impurity was then removed all other cross sections are low by ~0.26% (the N_2 impurity). The electrolytic oxygen used as the target gas in this experiment was purchased from the same source[10] as that used in previously reported experiments.[4,6] Since no attempt was made to remove a N_2 or H_2 impurity, cross sections measured in these experiments may be low by 0.52%.

The analyzing magnet used to determine the incident proton energy has been calibrated by Dagley *et al.*[11] The calibration constant is believed to be known to ±0.1%. However, sharp levels near $E_p=8$ MeV have been observed to shift as much as ±6 keV (±0.08%) from week to week. Therefore the incident proton energy is assigned an uncertainty of ±0.13%.

[10] General Dynamics Corporation, Liquid Carbonic Division, San Carlos, California.

[11] P. Dagley, W. Haeberli, and J. X. Saladin, Nucl. Phys. 24, 353 (1961).

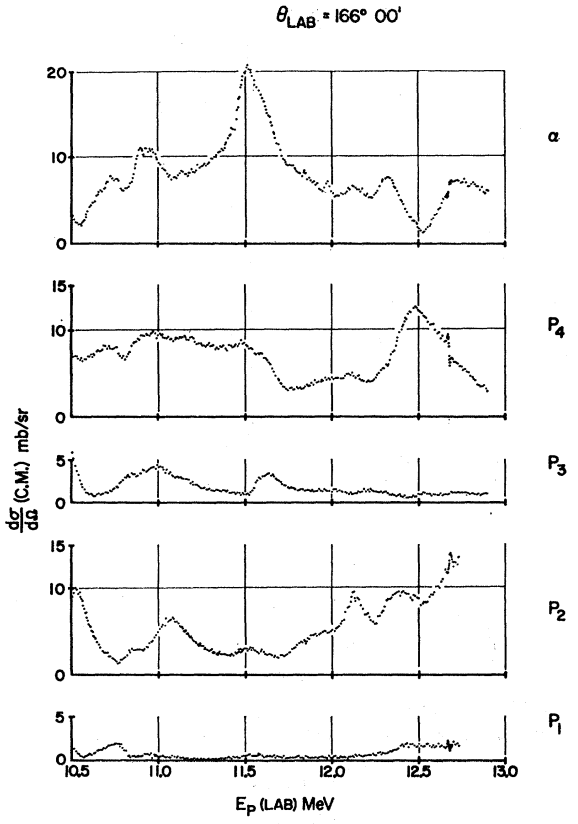

FIG. 9. Higher energy excitation curves at $\theta_{lab}=166°$. P_i refers to inelastic protons leaving O^{16} in its ith excited state and α refers to alphas leaving N^{13} in its ground state.

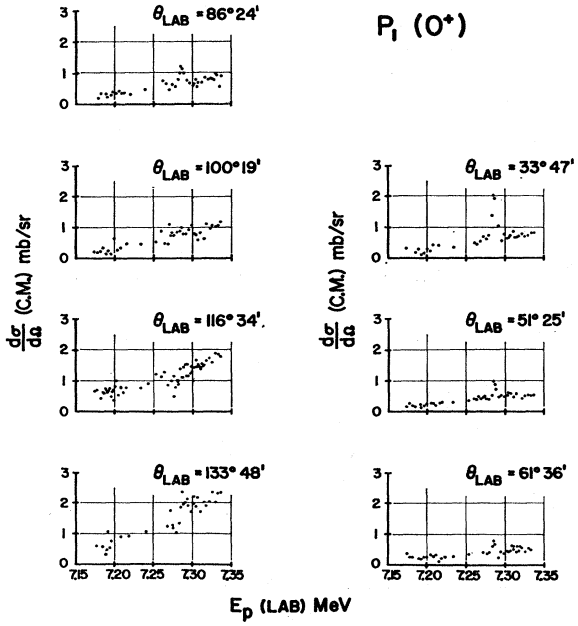

FIG. 10. Details of sharp structure from 7.15–7.35 MeV in excitation curves of protons leaving O^{16} in its first excited state.

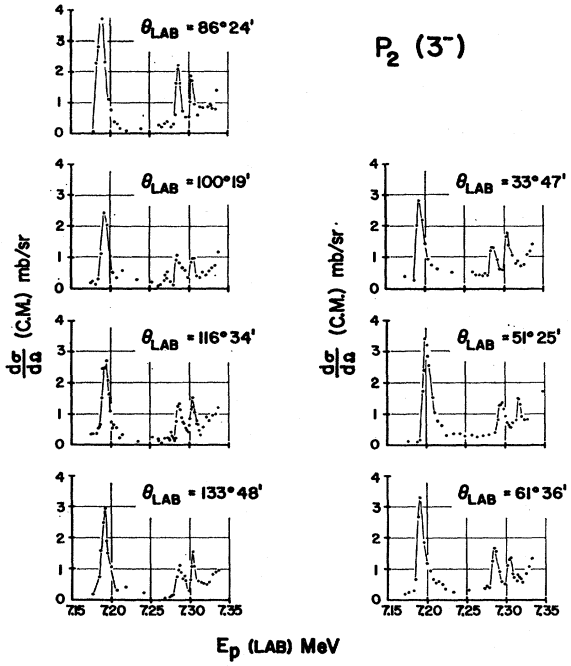

FIG. 11. Details of sharp structure from 7.15–7.35 MeV in excitation curves of protons leaving O^{16} in its second excited state.

Results

The excitation curves for $E_p \leqslant 10.5$ MeV are shown in Figs. 2–8. Figure 9 shows for all reaction groups the continuation of the $\theta_{lab}=166°$ excitation curve. For all of the data, the target thickness was $\leqslant 3$ keV. The data at $\theta_{lab}=166°$ were taken with energy steps $\leqslant 5$ keV, while at other angles the energy steps varied up to 23 keV depending upon the width of the resonant structure. Figures 10–12 display in greater detail the low-energy region where the earlier elastic scattering data[4] show four sharp resonances at $E_p=7.180$, 7.280, 7.287, and 7.305 MeV. Figures 13–18 show angular distributions taken every 8 keV near $E_p=8.3$ MeV where the

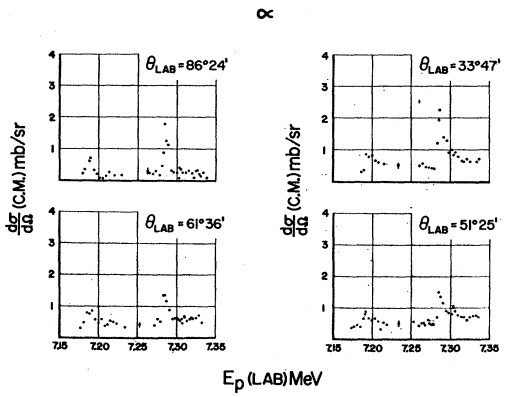

FIG. 12. Details of sharp structure from 7.15–7.35 MeV in excitation curves of alphas leaving N^{13} in its ground state.

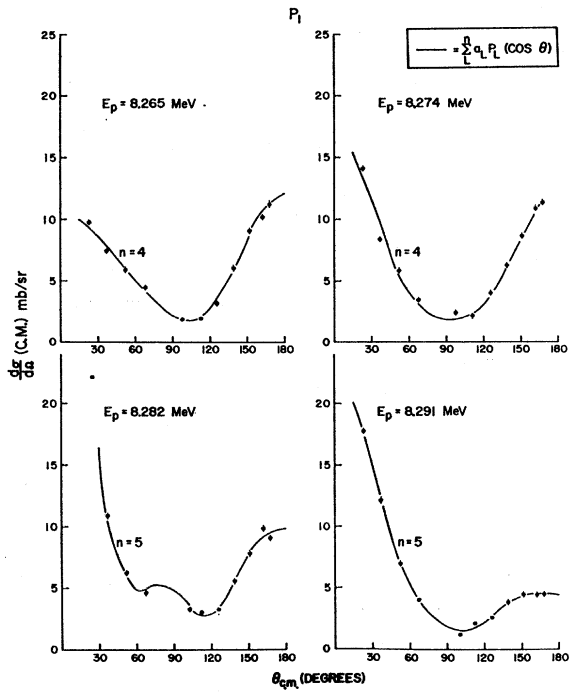

FIG. 13. Angular distributions over the doublet near $E_p = 8.3$ MeV for protons leaving O^{16} in its first excited state.

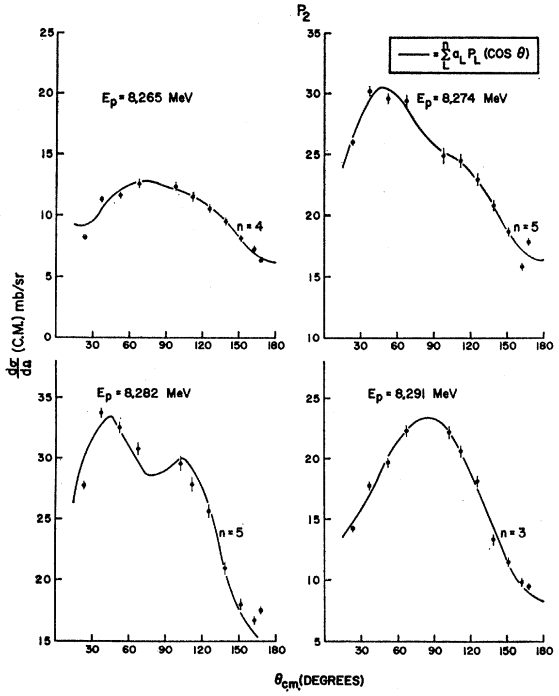

FIG. 15. Angular distributions over the doublet near $E_p = 8.3$ MeV for protons leaving O^{16} in its second excited state.

data of Figs. 2–8 (but especially Fig. 8) indicate several closely spaced and interfering levels. All error bars represent statistical uncertainties only.

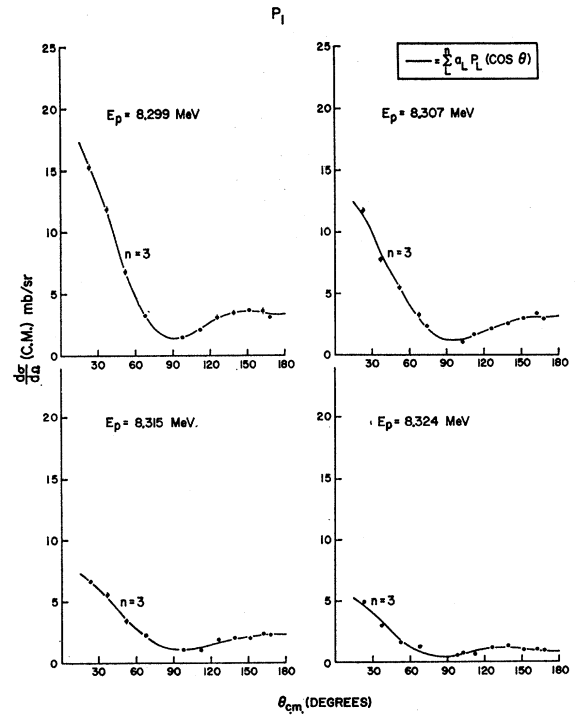

FIG. 14. Angular distributions over the doublet near $E_p = 8.3$ MeV for protons leaving O^{16} in its first excited state.

ANALYSIS

Theory

It is useful for purposes of analysis to express the center-of-mass differential cross section for a reaction

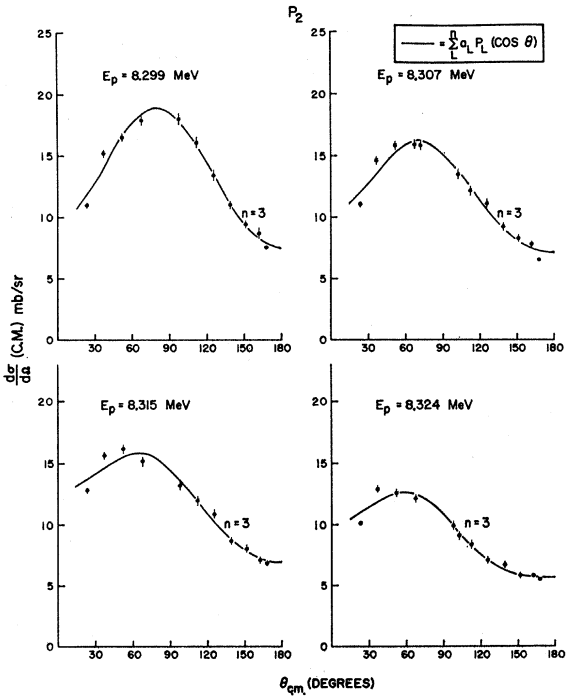

FIG. 16. Angular distributions over the doublet near $E_p = 8.3$ MeV for protons leaving O^{16} in its second excited state.

TABLE I. Nonvanishing products of $\bar{Z}$ coefficients of Legendre polynomials for $O^{16}(p,\alpha)N^{13}$ and $O^{16}(p,p_1)O^{16*}$ angular distributions.

J	$L=0$	$L=1$	$L=2$	$L=3$	$L=4$	$L=5$	$L=6$	$L=7$
Isolated levels								
$\frac{1}{2}$	2							
$\frac{3}{2}$	4		4					
$\frac{5}{2}$	6		48/7		36/7			
$\frac{7}{2}$	8		200/21		648/77		200/33	
Interfering levels; same parity								
$\frac{1}{2}$ $\frac{3}{2}$			4					
$\frac{1}{2}$ $\frac{5}{2}$			6					
$\frac{1}{2}$ $\frac{7}{2}$					8			
$\frac{3}{2}$ $\frac{5}{2}$			12/7		72/7			
$\frac{3}{2}$ $\frac{7}{2}$			72/7		40/7			
$\frac{5}{2}$ $\frac{7}{2}$			8/7		360/77		200/11	
Interfering levels; opposite parity (+) for $O^{16}(p,p_1)O^{16*}$ and (−) for $O^{16}(p,\alpha)N^{13}$								
$\frac{1}{2}$ $\frac{1}{2}$		±2						
$\frac{1}{2}$ $\frac{3}{2}$		±4						
$\frac{1}{2}$ $\frac{5}{2}$				±6				
$\frac{1}{2}$ $\frac{7}{2}$				±8				
$\frac{3}{2}$ $\frac{3}{2}$		±4/5		±36/5				
$\frac{3}{2}$ $\frac{5}{2}$		±36/5		±24/5				
$\frac{3}{2}$ $\frac{7}{2}$				±8/3		±40/3		
$\frac{5}{2}$ $\frac{5}{2}$		±18/35		±16/5		±100/7		
$\frac{5}{2}$ $\frac{7}{2}$		±72/7		±8		±40/7		
$\frac{7}{2}$ $\frac{7}{2}$		±8/21		±24/11		±600/91		±9800/429

in terms of the Legendre polynomials:

$$\frac{d\sigma}{d\Omega}(\alpha s;\alpha' s')=(2s+1)^{-1}k_\alpha^{-2}\sum_L B_L(\alpha s;\alpha' s')P_L(\cos\theta)\,. \quad (1)$$

This expression describes the differential cross section for a reaction proceeding from channel α with channel spin s to channel α' with channel spin s', k_α is the entrance-channel wave number, and θ is the center-of-mass angle.

For inelastic proton scattering leaving O^{16} in its first excited state (0^+), and for the (p,α) reaction leaving N^{13} in its ground state ($\frac{1}{2}^-$), the expression for B_L over an isolated level can be shown[12,13] to be simply

$$B_L=\bar{Z}(lJlJ,\tfrac{1}{2}L)\bar{Z}(l'Jl'J,\tfrac{1}{2}L)\frac{\Gamma_c\Gamma_{c'}}{\Gamma^2}\sin^2\delta\,, \quad (2)$$

where δ is the resonant phase shift. At every energy the ratio of the B_L's is equal to the ratio of the product of the $\bar{Z}$ coefficients.

In a region where two levels interfere, each B_L is the sum of the terms for isolated levels [Eq. (2)] and a term resulting from interference between the levels. The interference term for two levels denoted by λ and μ is[12,13]

$$\pm 2\bar{Z}(l_\lambda J_\lambda l_\mu J_\mu,\tfrac{1}{2}L)\bar{Z}(l_\lambda' J_\lambda l_\mu' J_\mu,\tfrac{1}{2}L)\left[\frac{\Gamma_{\lambda c}\Gamma_{\lambda c'}\Gamma_{\mu c}\Gamma_{\mu c'}}{\Gamma_\lambda\Gamma_\mu}\right]^{1/2}\times\sin\delta_\lambda\sin\delta_\mu\cos\Phi_{\lambda\mu}\,. \quad (3)$$

$\Phi_{\lambda\mu}=\delta_\lambda-\delta_\mu+\phi_{\lambda c}+\phi_{\lambda c'}-\phi_{\mu c}-\phi_{\mu c'}$, where the ϕ are potential phase shifts. Nonvanishing products of the $\bar{Z}$

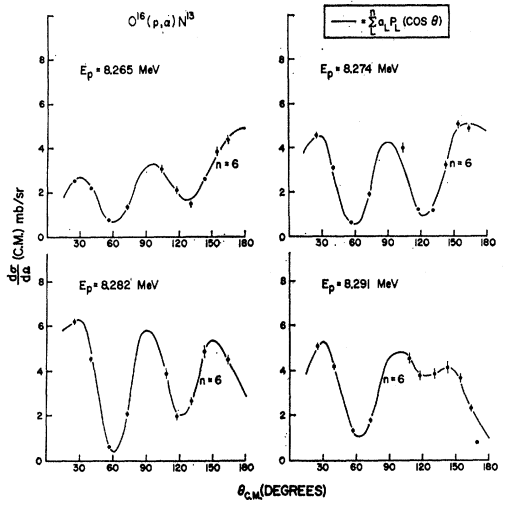

FIG. 17. Angular distributions over the doublet near $E_p=8.3$ MeV for alphas leaving N^{13} in its ground state.

[12] J. M. Blatt and L. C. Biedenharn, Rev. Mod. Phys. **24**, 258 (1952).

[13] A. M. Lane and R. G. Thomas, Rev. Mod. Phys. **30**, 257 (1958).

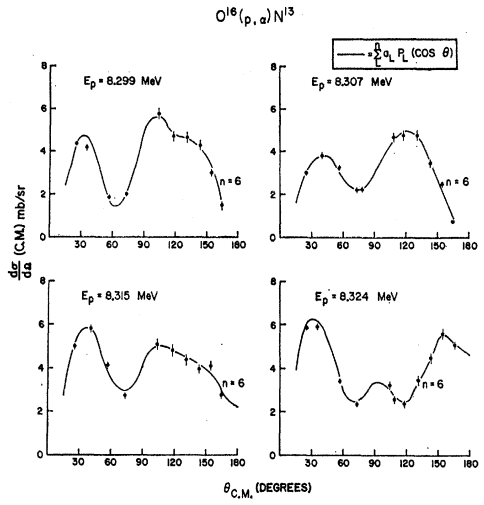

FIG. 18. Angular distributions over the doublet near $E_p = 8.3$ MeV for alphas leaving N^{13} in its ground state.

coefficients for both isolated and interfering levels are shown in Table I.[14,15]

For F^{17}, the sum over L in Eq. (1) is limited by the following conditions[12,13,16]:

$$L \leqslant 2l_{\max}, \quad L \leqslant 2l_{\max}', \quad L \leqslant 2J-1.$$

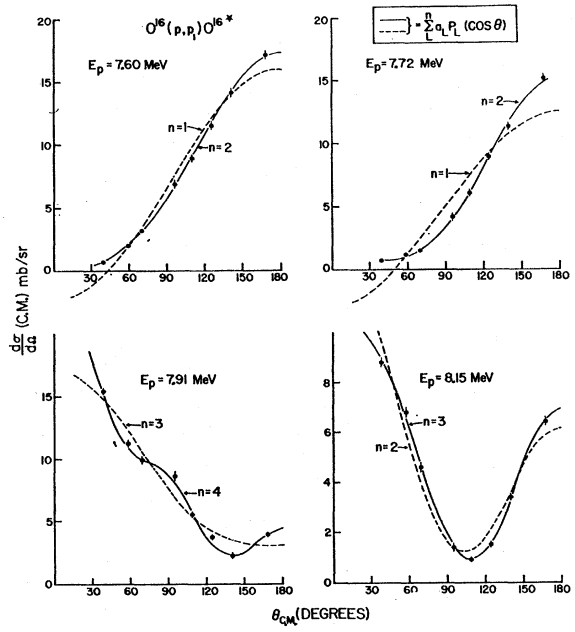

FIG. 19. Sample fits to angular distributions of inelastic protons leaving O^{16} in its first excited state.

[14] L. C. Biedenharn, Oak Ridge National Laboratory Report, ORNL-1501 (unpublished).

[15] The $\bar{Z}$ coefficients used here are related to the Z coefficients in Ref. 12 by $\bar{Z}(l_\lambda J_\lambda l_\mu J_\mu, SL) = i^{l_\lambda - l_\mu + L} Z(l_\lambda J_\lambda l_\mu J_\mu, SL)$.

[16] J. M. Blatt and V. F. Weisskopf, *Theoretical Nuclear Physics* (John Wiley & Sons, Inc., New York, 1962), p. 540.

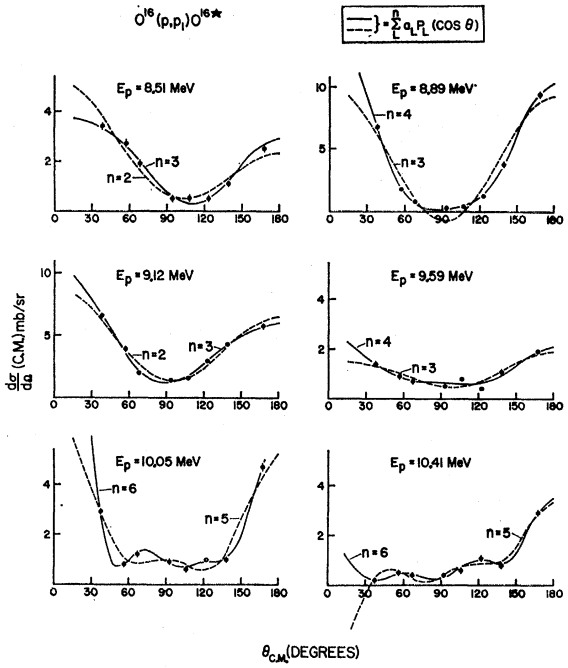

FIG. 20. Sample fits to angular distributions of inelastic protons leaving O^{16} in its first excited state.

Procedure

Angular distributions were chosen from the excitation curves and fitted with a sum of Legendre polynomials using an IBM-704 computer. The program minimized

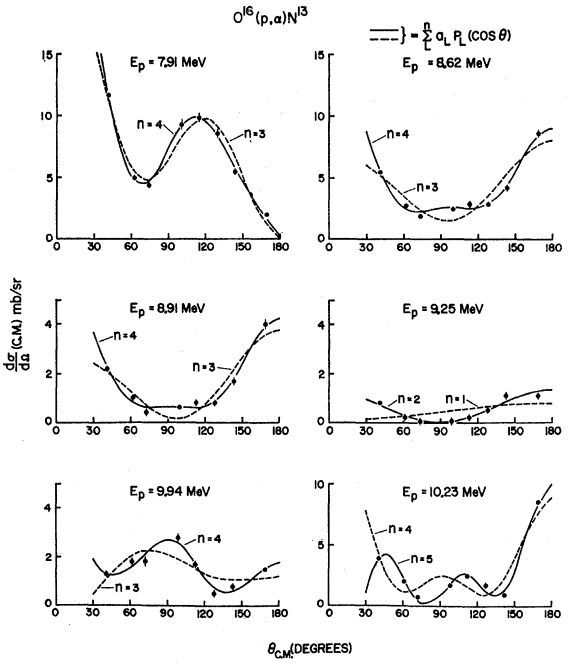

FIG. 21. Sample fits to angular distributions of alphas leaving N^{13} in its ground state.

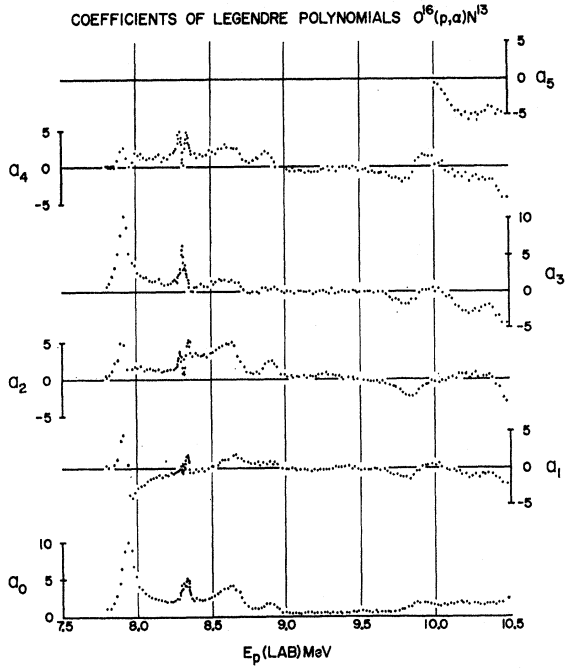

FIG. 22. Extracted coefficients of Legendre polynomials for angular distributions of alphas leaving N^{13} in its ground state.

the quantity

$$\chi^2=\sum_{i=1}^{N}\left[\sum_{L=0}^{n}a_L P_L(\cos\theta_i)-\left(\frac{d\sigma}{d\Omega}\right)_i\right]^2,$$

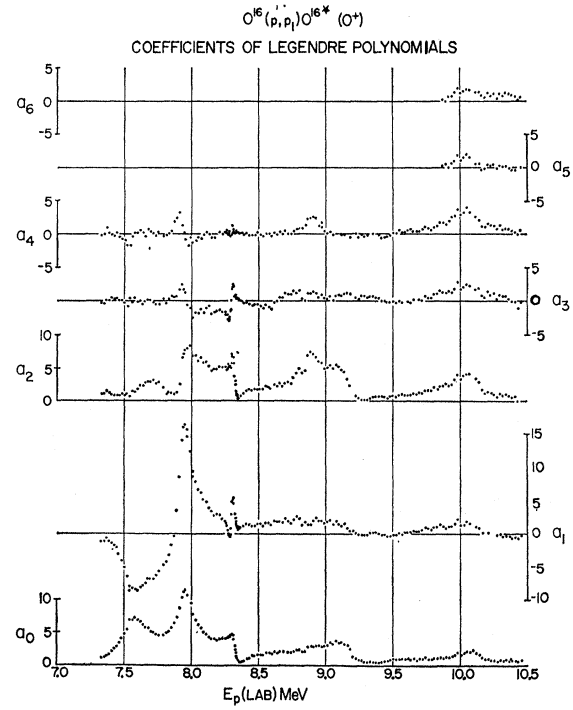

FIG. 23. Extracted coefficients of Legendre polynomials for angular distributions of inelastic protons leaving O^{16} in its first excited state.

where N is the number of experimental points to be fitted, and n is the highest degree Lengendre polynomial used. Sample fits to the experimental data are shown in Figs. 19–21. The required a_L's are shown as a function of energy in Figs. 22–25. Coefficients obtained by fitting the angular distributions taken over the sharp structure near $E_p=8.3$ MeV are shown in Figs. 26 and 27.

Spin Assignments

As can be seen in Figs. 22 and 23, coefficients are nonzero through a_4 for both p_1 and the alphas over the level at $E_p=7.94$ MeV. If we treat the level as isolated, then Table I requires $J=\frac{5}{2}$. However, the nonzero a_1

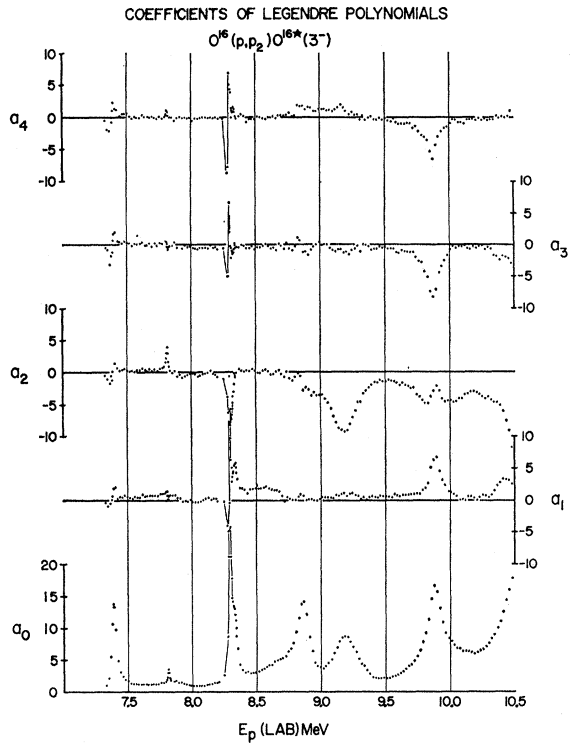

FIG. 24. Extracted coefficients of Legendre polynomials for angular distributions of inelastic protons leaving O^{16} in its second excited state.

and a_3 over the resonance imply interference between the level at 7.94 MeV and a level of opposite parity, and $J=\frac{3}{2}$ (again see Table I). There is evidence in the a_0 curves for p_1 and the alphas (see Figs. 22 and 23) for a broad level ($\Gamma\sim750$ keV) near $E_p=8.1$ MeV. This broad level is assumed to be the interfering opposite parity $J=\frac{3}{2}$ level required to give the a_1 and a_3 coefficients at 7.94 MeV. Such a level would also contribute directly to the nonzero a_2 coefficient seen near $E_p=7.7$ and 8.2 MeV in the p_1 angular distributions (see Fig. 23). The large a_1 and a_3 present in p_1 angular distributions over the level at $E_p=7.58$-MeV (see Fig. 23) can be explained by assigning the 7.58-MeV level a

$J=\frac{1}{2}$ with parity opposite that of the postulated broad $J=\frac{3}{2}$ level at 8.1 MeV (see Table I). The maximum in a_2 near $E_p=7.7$ MeV is not from the level at 7.58 MeV since it is shifted to a higher energy. This a_2 is from the broad $J=\frac{3}{2}$ level as previously mentioned and the minimum in a_2 near $E_p=7.9$ MeV is probably caused by interference between the $J=\frac{1}{2}$ level at 7.58 MeV and the $J=\frac{5}{2}$ level at 7.94 MeV which have the same parity.

Angular distributions over the level seen in the alpha data at $E_p=8.63$ MeV require coefficients through a_4 (see Fig. 22). This level is therefore assigned $J=\frac{5}{2}$. The nonzero a_1 and a_3 are again explained by assuming the level has parity opposite that of the broad interfering $J=\frac{3}{2}$ level at 8.1 MeV. The observed ratios $a_2/a_0=5/4$ and $a_4/a_0=3/4$ are in good agreement with the theoreti-

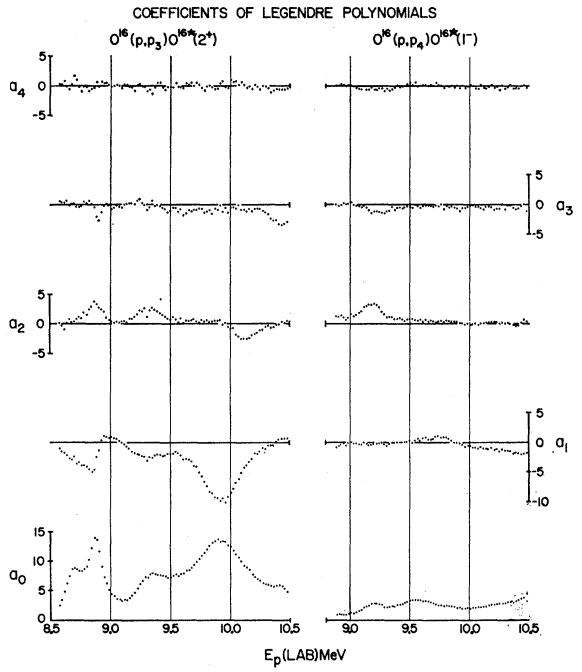

FIG. 25. Extracted coefficients of Legendre polynomials for angular distributions of inelastic protons leaving O^{16} in its third and fourth excited state.

cal ratios of the products of the $\bar{Z}$ coefficients for an isolated $J=\frac{5}{2}$ level, $a_2/a_0=8/7$ and $a_4/a_0=6/7$.

Baldinger *et al.*[17] have reported a broad level ($\Gamma\sim750$ keV) at $E_x=7.72$ MeV in O^{17} with a spin and parity of $\frac{3}{2}^-$. The broad level at $E_x=8.2$ MeV ($E_p=8.1$ MeV) in F^{17} is assumed to be the mirror of the level in O^{17} reported by Baldinger *et al.* This assumption permits the assignment of absolute parities to levels which interfere with the broad level at 8.1 MeV. The spin and parity assignments are then: 7.58, $\frac{1}{2}^+$; 7.94, $\frac{5}{2}^+$; 8.1, $\frac{3}{2}^-$; 8.63, $\frac{5}{2}^+$.

The angular distributions shown in Figs. 13–18 were

[17] E. Baldinger, P. Huber, and W. G. Proctor, Helv. Phys. Acta 25, 142 (1952).

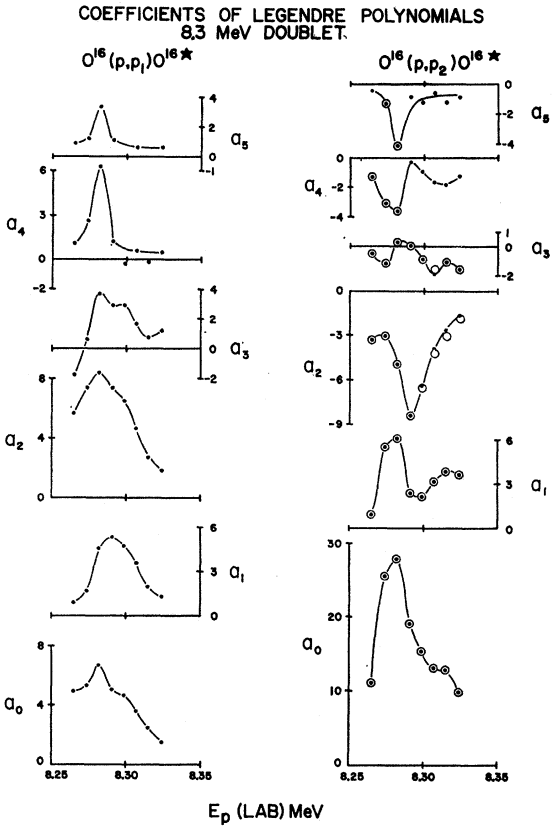

FIG. 26. Extracted coefficients of Legendre polynomials for angular distributions shown in Figs. 13–16. Solid dots are coefficients obtained when all polynomials through $n=6$ are used. (However, a_6 is small and not plotted.) Open circles are coefficients when only polynomials up to that required to fit the data are used.

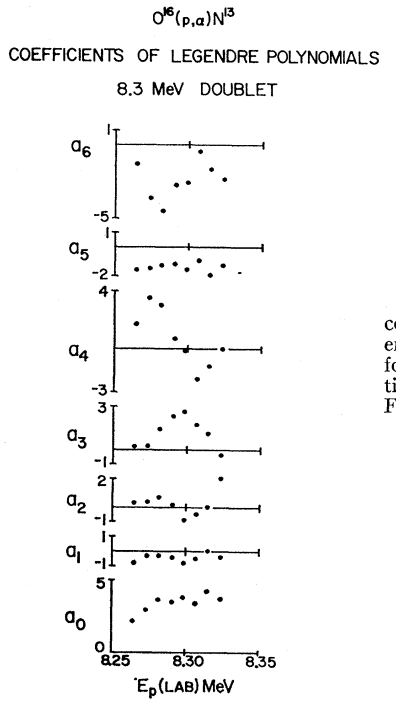

FIG. 27. Extracted coefficients of Legendre polynomials for angular distributions shown in Figs. 17 and 18.

TABLE II. Reduced widths for F^{17} levels.[a]

E_p (MeV)	J	π	$\gamma_{p_0}^2\times10^{12}$ (keV-cm)	$\gamma_{p_0}^2/\Delta p$	$\gamma_{p_1}^2\times10^{12}$ (keV-cm)	$\gamma_{p_1}^2/\Delta p$	$\gamma_\alpha^2\times10^{12}$ (keV-cm)	$\gamma_\alpha^2/\Delta\alpha$
7.58	$\frac{1}{2}$	+	14.2	0.011	41.6	0.032	31.2	0.087
			4.37	0.0033	136	0.10	102.2	0.28
		(−)	17.0	0.013	113	0.086	18.8	0.052
			5.20	0.0040	372	0.28	61.2	0.17
7.94	$\frac{5}{2}$	+	*13.6*	*0.010*	*111*	*0.085*	*148*	*0.41*
			4.12	0.0032	368	0.28	497	(1.4)
		(−)	28.8	0.022	2120	(1.6)	42.1	0.12
			8.66	0.0066	6940	(5.3)	146	0.41
8.1	$\frac{3}{2}$	(+)	105	0.080	336	0.26	22.2	0.062
			12.3	0.0094	2870	(2.2)	190	0.53
		−	*75.2*	*0.058*	*57.7*	*0.044*	*54.9*	*0.15*
			8.8	0.0067	494	0.38	468	(1.3)
8.27	$\frac{5}{2}$	(+)	1.12	0.00086	3.30	0.0025	1.84	0.0051
			0.665	0.00051	5.60	0.0043	3.11	0.0086
		−	2.24	0.0017	45.3	0.035	0.58	0.0016
			1.33	0.0010	77.1	0.059	0.98	0.0027
8.31	$\frac{7}{2}$	+	*43.2*	*0.033*	*317*	*0.24*	*5.72*	*0.016*
			5.48	0.0042	2460	(1.9)	43.9	0.12
		(−)	12.1	0.0093	13.7	0.010	28.5	0.079
			1.53	0.0012	107	0.082	215	0.60
8.63	$\frac{5}{2}$	+	26.8	0.021			13.4	0.037
			2.10	0.0016			165	0.46
		(−)	52.0	0.040			4.89	0.014
			4.09	0.0031			60.6	0.17
8.88	$\frac{5}{2}$	(+)	9.67	0.0074	5.88	0.0045	3.75	0.010
			8.38	0.0064	6.76	0.0052	4.36	0.012
		−	18.5	0.014	55.5	0.042	1.51	0.0042
			16.0	0.012	64.0	0.049	1.76	0.0049
9.10	$\frac{3}{2}$	+	*26.1*	*0.020*	*12.2*	*0.0093*		
			1.10	0.00084	292	0.22		
		(−)	19.2	0.015	3.38	0.0026		
			0.81	0.00062	80.7	0.062		
10.04	$\frac{7}{2}$	+	173	0.13	189	0.14		
			2.54	0.0019	12700	(9.7)		
		−	61.3	0.047	16.7	0.013		
			0.90	0.00069	1130	0.86		

[a] Two solutions are given for each assumed parity. Less likely values are in parenthesis and preferred solutions in italics.

$\Delta p=\frac{3}{2}(\hbar^2/\mu a)=1307\times10^{-12}$ keV-cm ($a=5.11$f).
$\Delta\alpha=\frac{3}{2}(\hbar^2/\mu a)=360\times10^{-12}$ keV-cm ($a=5.72$f).

taken over the sharp structure near $E_p=8.3$ MeV because it was felt that small energy shifts of the accelerator could distort angular distributions chosen from the excitation curves. The analysis of the two levels ($E_p=8.27$ and 8.31 MeV) seen in this region is based on these angular distributions. The presence of the nonzero a_6 required to fit the alpha data in this region (Fig. 27) requires that at least one of the two sharp levels has $J=\frac{7}{2}$. On the basis of the p_1 data in this region (Fig. 26), the level at 8.27 MeV is assigned $J=\frac{5}{2}$. This assignment then requires that the level at 8.31 MeV has $J=\frac{7}{2}$ in order to account for the nonzero a_6 needed to fit the alpha data. The level at $E_p=8.31$ MeV must have a very small particle width for decay via p_1, as it is scarcely detectable in the p_1 data (Fig. 2). Consequently, it is not surprising that no a_6 is needed for the p_1 data. The nonzero a_5 required to fit one of the p_1 angular distributions (Fig. 26) may be caused by interference between the $J=\frac{5}{2}$ level at 8.27 MeV and another $J=\frac{5}{2}$ level of opposite parity. If the interfering level is the $J^\pi=\frac{5}{2}^+$ level at 7.94 MeV, the level at 8.27 MeV is then $J^\pi=\frac{5}{2}^-$. The fact that the a_6 needed to fit the alpha data in this region are negative can only be accounted for by interference between the $J=\frac{7}{2}$ level at 8.31 MeV and another level of the same parity having $J=\frac{5}{2}$. If the two members of the doublet have the same parity this might explain the negative a_6. However, since the level at 8.27 MeV is quite narrow, it appears unlikely that the interference would be strong enough at the higher energies to produce a negative a_6. It is more likely that the negative a_6 is caused by interference with the $\frac{5}{2}^+$ level at 8.63 MeV. This interference would assign a positive parity to the $\frac{7}{2}$ level at 8.31 MeV.

Since coefficients through a_4 are required over the level at $E_p=8.88$ MeV for both the p_1 and alpha data (Figs. 22 and 23), the level is assigned $J=\frac{5}{2}$. Angular distributions for p_2 over this level are nearly isotropic (see Fig. 24). Since neither l or $2J-1$ can be zero, this implies that $l'=0$ and hence the proton decay to the 3^- level of O^{16} is largely via s waves. Therefore the level at 8.88 MeV is assigned a negative parity.

The level seen in the p_1 data at $E_p=9.10$ MeV has nonzero coefficients only through a_2 and hence is assigned $J=\frac{3}{2}$. The nonzero a_1 and a_3 coefficients over

TABLE III. Energy levels in F^{17}. It should be noted that for levels at $E_p > 10.5$ MeV the approximate resonant energies and lab widths were obtained only from the $\theta_{lab} = 166°$ excitation curves and are considered to be quite uncertain.

E_p(MeV)	E_x(MeV)	Γ_{lab}(keV)	J^π	Resonating groups
7.186	7.359	10±2		$p_0p_2\alpha$
7.280	7.448	<5		p_0
7.286	7.453	7±2		$p_0p_1p_2\alpha$
7.304	7.470	5±2		p_0p_2
7.313	7.479	845	$\frac{3}{2}^{+a}$	p_0
7.39	7.55	40±5	$\frac{7}{2}^{-a}$	p_0p_2
7.58	7.73	190±30	$\frac{1}{2}^{+b}$	$p_0p_1\alpha$
7.81	7.95	10±3		p_2
7.89	8.02	50±20		$p_0\alpha$
7.94	8.07	110±20	$\frac{5}{2}^{+b}$	$p_0p_1\alpha$
8.1	8.2	750±250	$\frac{3}{2}^{-b}$	$(p_0)p_1\alpha$
8.27	8.38	12±5	$\frac{5}{2}^{-b}$	$p_0p_1p_2p_3\alpha$
8.31	8.42	45±10	$\frac{7}{2}^{+b}$	$p_0p_1p_2p_3\alpha$
8.63	8.72	200±30	$\frac{5}{2}^{+b}$	$p_2\alpha^c$
8.70	8.78	160±20		p_3p_4
8.88	8.95	130±20	$\frac{5}{2}^{-}$	$p_0p_1p_2p_3p_4\alpha$
9.10	9.16	200±50	$\frac{3}{2}^{+}$	$p_0p_1^c$
9.20	9.26	220±40		$p_2p_4\alpha$
9.35	9.40	250±100		p_3
9.59	9.62	330±75		$p_0p_1p_4$
9.87	9.89	140±20		$p_0p_2\alpha$
9.92	9.93	450±100		p_3
10.04	10.05	300±100	$\frac{7}{2}$	p_0p_1
10.23	10.22	270±85		α
10.42	10.40	170±40		p_1p_3
10.52	10.50	150±30		$p_0p_2\alpha$
10.74	10.70	150±30		$p_1\alpha$
10.83	10.79	130±40		$p_0p_2(p_3)(\alpha)$
11.00	10.95	200±50		$(p_2)p_3(\alpha)$
11.52	11.44	260±60		$p_2\alpha$
11.64	11.55	170±30		p_3^c
11.73	11.64	160±40		p_0
11.89	11.79	200±100		p_2
11.98	11.87	40±20		α
12.12	12.00	130±40		$p_2\alpha$
12.32	12.19	170±60		$\alpha(p_2)$
12.39	12.26	200±50		p_0p_2
12.49	12.35	280±50		p_1p_4
12.671	12.522	≤5		$p_0p_1p_2p_4\alpha$
13.215	13.034	≤5		p_0

[a] J^π from Ref. 5.
[b] Parity from interference with broad level at $E_p = 8.1$ which is assumed to be $3/2^-$.
[c] Bracketed energy levels: In several cases, different reaction channels show broad resonances at slightly different energies. It is not always clear whether these resonances correspond to different F^{17} states or whether the energy for peak cross sections has been shifted (by penetration factors or interference effects) and the resonances in all channels arise from the same F^{17} state. In such cases the neighboring resonances have been bracketed.

the 8.88- and 9.10-MeV levels can be explained if the levels have opposite parity. Therefore, the 9.10-MeV level is assigned positive parity.

Since coefficients through a_6 are required to fit the p_1 angular distributions over the level at 10.04 MeV (Fig. 23), the level is assigned $J = \frac{7}{2}$.

Reduced Widths

For protons on O^{16} at the resonant energy of an isolated level of spin J the total cross section for a given reaction channel (ν) can be written as

$$\sigma_\nu = 4\pi\Delta a_{0\nu} = 2\pi k^{-2}(2J+1)\Gamma_{p_0}\Gamma_\nu\Gamma^{-2}, \quad (4)$$

where Γ_{p_0} is the partial width for the elastic channel, Γ_ν is the partial width for the reaction channel, and $\Delta a_{0\nu}$ is the contribution to $a_{0\nu}$ from the level. Since $\Gamma = \Gamma_{p_0} + \sum_\nu \Gamma_\nu$, the total reaction cross section can be written

$$\sigma_{total} = 4\pi\sum_\nu \Delta a_{0\nu} = 2\pi k^{-2}(2J+1)\Gamma_{p_0}(\Gamma - \Gamma_{p_0})\Gamma^{-2}. \quad (5)$$

If it is assumed that the present measurements cover all important open channels, then Eq. (5) can be solved for two values of Γ_{p_0} and each of these can be used in Eq. (4) to calculate the other partial widths. When J^π is known, reduced widths can then be calculated for p_1 and the alphas using $\gamma_\nu^2 = \frac{1}{2}\Gamma_\nu k^{-1}A_l^{-2}$, where A_l^{-2} is the penetrability factor. The reduced widths for both solutions to Eqs. (4) and (5) are shown in Table II. Since the parity assignments are somewhat doubtful, values corresponding to both parities are shown. In cases where one of the solutions is clearly preferred it is italicized. Unlikely values are in parentheses.

CONCLUSIONS

Table III shows a complete list of the levels found in F^{17} in the energy range $E_x = 7.0$–13.0 MeV. Information about levels found in elastic scattering data is taken from Refs. 5 and 6. The resonant energies, widths, and uncertainty in widths shown in the table are the best values that can be assigned on the basis of all available information. When possible, the energies and widths were taken from the a_0 curves. Because only levels of the same spin and parity interfere in a_0, interference effects should be a minimum here.

Figure 28 shows energy level diagrams for F^{17} and O^{17}. F^{17} levels are those listed in Table III. Mirror levels

TABLE IV. Comparison of O^{17} and F^{17} level parameters.

O^{17}					F^{17}				
E_x(MeV)	J^π	$\Gamma_{c.m.}$(keV)	$\gamma_{n_0}^2/(3\hbar^2/2\mu a)$[a]	$\gamma_\alpha^2/(3\hbar^2/2\mu a)$[a]	E_x(MeV)	J^π	$\Gamma_{c.m.}$(keV)	$\gamma_{p_0}^2/(3\hbar^2/2\mu a)$	$\gamma_\alpha^2/(3\hbar^2/2\mu a)$
7.56	$\geq\frac{7}{2}$	≤4			7.55	$\frac{7}{2}^-$	38	0.00882[b]	
7.72	$\frac{3}{2}^{-c}$	750			8.2	$\frac{3}{2}^-$	706	0.058	0.15
8.39	$\frac{5}{2}^{-c}$	11	0.0073	0.0036	8.38	$\frac{5}{2}^-$	11	0.0010	0.0027
								0.0017	0.0016
8.46	$\frac{7}{2}^{+c}$	9	0.049	0.0039	8.42	$\frac{7}{2}^+$	42	0.033	0.016
8.88	$\frac{3}{2}$	110	0.016	0.033	9.16	$\frac{3}{2}^+$	188	0.020	<0.010

[a] R. B. Walton, J. D. Clement, and F. Boreli, Phys. Rev. 107, 1065 (1957).
[b] See Ref. 5.
[c] Parity assignment from $C^{13}(\alpha,\alpha)C^{13}$. See reference in caption of Fig. 28.

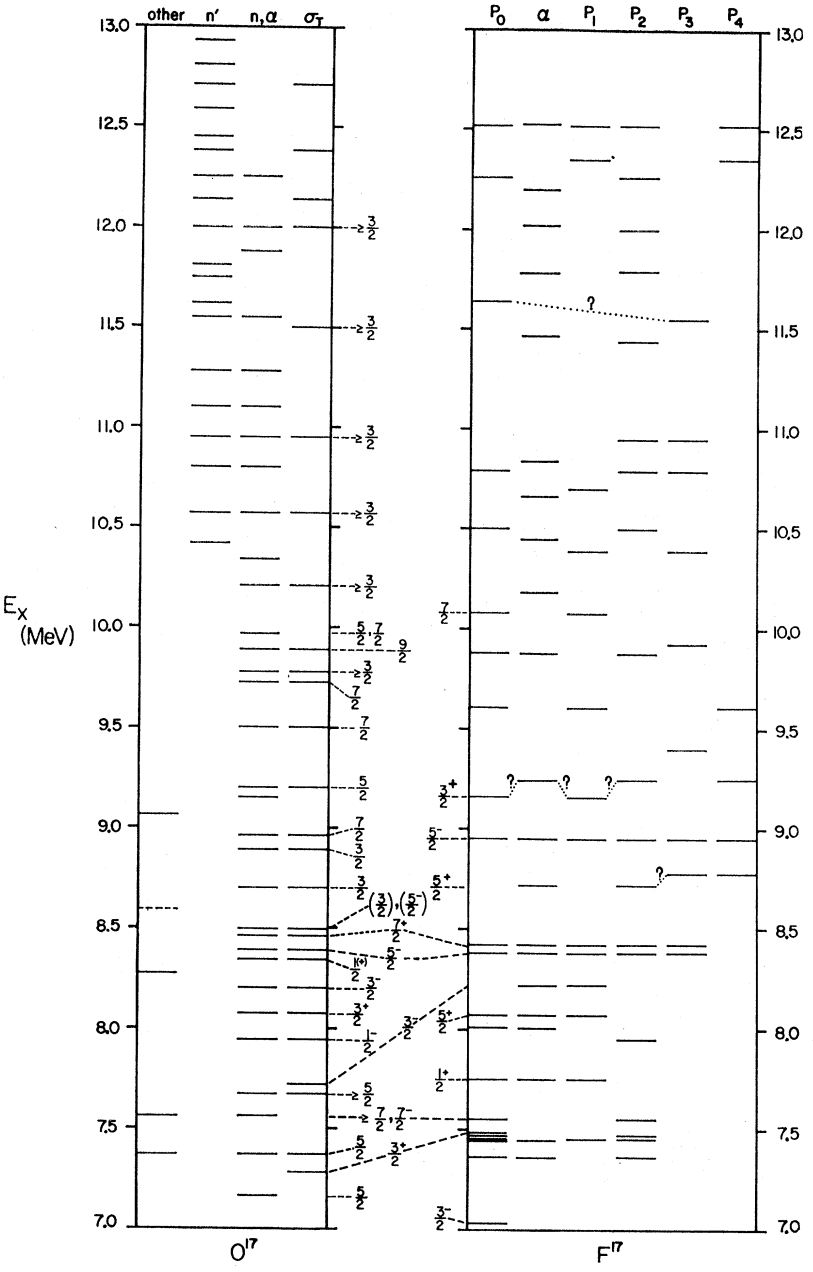

FIG. 28. Comparison of energy levels of O^{17} and F^{17} from 7–13 MeV. Information about O^{17} levels are from a compilation by F. Ajzenberg-Selove and T. Lauritsen, Nucl. Phys. **11**, 1 (1959), except (a) levels under n' are from inelastic scattering work by H. E. Hall and T. W. Bonner, *ibid.* **14**, 295 (1959) and $C^{13}(\alpha,n\gamma)O^{16}$ work by R. H. Spear, J. D. Larson, and J. D. Pearson, *ibid.* **41**, 353 (1963); (b) levels under (n,α) include work by D. M. Worley, Jr., R. Bass, T. W. Bonner, E. A. Davis, and F. Gabbard, Bull. Am. Phys. Soc. **5**, 109 (1960); (c) levels under σ_T include work by D. B. Fossan, R. L. Walter, W. E. Wilson, and H. H. Barschall, Phys. Rev. **123**, 209 (1961); and (d) parity assignments to levels from 7.94–8.49 MeV are from $C^{13}(\alpha,\alpha)C^{13}$ work of B. K. Barnes, R. L. Steele, T. A. Belote, and J. R. Risser, Bull. Am. Phys. Soc. **8**, 125 (1963). The F^{17} levels connected by a dotted line (?) are inferred from broad resonances seen in different reaction groups. Interference and penetrability effects may possibly account for the differences in resonant energy and hence these groups may arise from the same F^{17} state.

in O^{17} and F^{17} are connected with dashed lines in Fig. 28. The correspondence between the $\frac{3}{2}^+$ levels near $E_x=7.4$ MeV was made by Salisbury and Richards.[5] The $\frac{7}{2}$ levels at 7.55 MeV are considered to be mirror levels solely on the basis of the spins and similarity in excitation energies since the O^{17} reduced width is unknown. It was assumed in this analysis that the $\frac{3}{2}^-$ level at7.72 MeV in O^{17} and the $\frac{3}{2}$ level at 8.2 MeV in F^{17} are mirror levels. This assumption was based on the similarity in total widths for the levels. It must be emphasized that all parity assignments made in this paper except those to the levels at $E_x=8.95$ and 9.16 MeV are based on this assumption. Table IV shows parameters on which the other correspondences in Fig. 28 are based.

ACKNOWLEDGMENTS

We wish to express our thanks to Professor Hugh T. Richards for his continued encouragement and advice throughout this experiment. Illuminating discussions with Professor C. H. Blanchard concerning the theory used in the analysis are gratefully acknowledged. The aid of R. E. Rothe, J. Jobst, and D. R. Croley in collecting the data and maintaining the equipment is appreciated.